

# Fractional Talbot effect for periodic microlens arrays

**Brigitte Besold**  
**Norbert Lindlein**  
 Universität Erlangen-Nürnberg  
 Physikalisches Institut  
 Lehrstuhl für Optik  
 Staudtstraße 7/B2  
 Erlangen D-91058, Germany  
 E-mail: norbert@move.physik.uni-erlangen.de

**Abstract.** It is well known that the foci of a periodic array of microlenses are reproduced and multiplied in the fractional Talbot planes. But the intensity between the multiplied foci varies in general in one period, especially if the light in the spacing between the lenses is not absorbed but transmitted. Additionally, in the case of microlenses with a high numerical aperture the parabolic approximation or Fresnel diffraction, which is normally used to explain the Talbot effect, is no longer valid. A theoretical explanation and numerical simulations are given together with experimental results. © 1997 Society of Photo-Optical Instrumentation Engineers. [S0091-3286(97)02904-8]

Subject terms: fractional Talbot effect; microlens arrays; self-imaging; intensity of foci; array illuminator; propagation of angular spectrum.

Paper 30096 received Sep. 23, 1996; accepted for publication Dec. 3, 1996.

## 1 Introduction

The Talbot effect and the fractional Talbot effect or, which is the same, the so-called self-imaging properties of periodic structures either with 1-D or 2-D periodicity, which are illuminated by a coherent plane wave is a well-known optical phenomenon,<sup>1,2</sup> which demonstrates very well the wave nature of light. The foci of a 2-D periodic array of microlenses also form a periodic structure and therefore the foci are reproduced in the Talbot planes and are multiply reproduced in the fractional Talbot planes.<sup>3</sup> If walk-off effects due to the finite size of the microlens array and blurring of the foci due to their finite numerical aperture (high spatial frequencies) can be neglected, the intensity of the foci in the Talbot planes is the same as in the original focal plane. The foci are multiplied in the fractional Talbot planes in general. But the intensity of the multiplied foci varies in one period if certain conditions are valid. This is, of course, not desirable if the multiplied foci will be used as array illuminators.<sup>4,5</sup> Therefore, theoretical analytic considerations (Sec. 2) as well as numerical simulations (Sec. 3) for the fractional Talbot effect at periodic microlens arrays are given in this paper. The numerical simulations are also valid for lenses with quite high numerical aperture (i.e., large spatial frequencies). Some experimental results, which are in quite good agreement with the numerical simulations, are presented in Sec. 4.

## 2 Analytic Expressions for the Intensity of the Foci in the Fractional Talbot Planes

An array of microlenses that is periodic in the two orthogonal directions  $x$  and  $y$  with the period  $p$  is illuminated by a plane wave. It is assumed in the following that the array is infinitely extended or in practice that it is so large that walk-off effects can be neglected. The foci in the focal plane of the microlens array at  $z=0$  then also form a periodic array. The coordinate system used is shown in Fig. 1. The complex wave amplitude  $u(x,y,z=0)$  of the foci can be represented by the convolution of the wave amplitude  $A(x,y)$  of a single focus and the array generating function  $g(x,y)$ :

$$u(x,y,z=0) = A(x,y) \otimes g(x,y), \quad (1)$$

with

$$g(x,y) = \sum_{k=-\infty}^{+\infty} \sum_{l=-\infty}^{+\infty} \delta(x-kp) \delta(y-lp). \quad (2)$$

The symbol  $\otimes$  is used to indicate a convolution between two functions:

$$A(x,y) \otimes g(x,y) = \int_{-\infty}^{+\infty} \int_{-\infty}^{+\infty} A(x',y') g(x-x', y-y') dx' dy'. \quad (3)$$

The amplitude function in a plane parallel to the focal plane at  $z=z_0$  can be calculated with the method of the propagation of the angular spectrum of plane waves<sup>6</sup>:

$$u(x,y,z=z_0) = \int_{-\infty}^{+\infty} \int_{-\infty}^{+\infty} \tilde{u}(v_x,v_y) \exp\left\{2\pi i \frac{z_0}{\lambda} [1 - \lambda^2(v_x^2 + v_y^2)]^{1/2}\right\} \exp[2\pi i(v_x x + v_y y)] dv_x dv_y, \quad (4)$$

where  $\lambda$  is the wavelength of the light,  $v_x$  and  $v_y$  are spatial frequencies and the function  $\tilde{u}(v_x,v_y)$  is the Fourier transform of  $u(x,y,z=0)$ :

$$\tilde{u}(v_x,v_y) = \int_{-\infty}^{+\infty} \int_{-\infty}^{+\infty} u(x,y,z=0) \times \exp[-2\pi i(v_x x + v_y y)] dx dy. \quad (5)$$

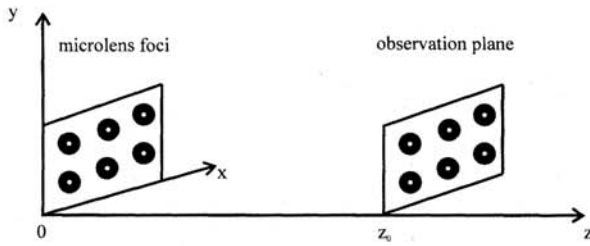


Fig. 1 Coordinate system.

By applying the convolution theorem of Fourier mathematics and using Eqs. (1) and (2),  $u(x, y, z = z_0)$  can be written as

$$u(x, y, z = z_0) = A(x, y) \otimes G(x, y, z = z_0), \quad (6)$$

with

$$G(x, y, z = z_0) = \int_{-\infty}^{+\infty} \int_{-\infty}^{+\infty} \tilde{g}(v_x, v_y) \times \exp\left\{2\pi i \frac{z_0}{\lambda} [1 - \lambda^2(v_x^2 + v_y^2)]^{1/2}\right\} \times \exp[2\pi i(v_x x + v_y y)] dv_x dv_y, \quad (7)$$

The Fourier transform  $\tilde{g}$  of  $g$  can be calculated by developing  $g$  into a Fourier series:

$$g(x, y) = \sum_{k=-\infty}^{+\infty} \sum_{l=-\infty}^{+\infty} \delta(x - kp) \delta(y - lp) = \frac{1}{p^2} \sum_{m=-\infty}^{+\infty} \sum_{n=-\infty}^{+\infty} \exp\left(2\pi i \frac{mx + ny}{p}\right), \quad (8)$$

and using the identity for  $\delta$  functions:

$$\int_{-\infty}^{+\infty} \exp[2\pi i(a - v)x] dx = \delta(a - v). \quad (9)$$

Thus, the result is

$$\tilde{g}(v_x, v_y) = \frac{1}{p^2} \sum_{k=-\infty}^{+\infty} \sum_{l=-\infty}^{+\infty} \delta\left(\frac{k}{p} - v_x\right) \delta\left(\frac{l}{p} - v_y\right). \quad (10)$$

It is well known that self-imaging in the normal meaning occurs only if the function  $\bar{u}$  has values considerably different from zero only for small spatial frequencies<sup>2</sup> ( $v_x^2 + v_y^2 \ll 1/\lambda^2$ ). In this case, the square roots of Eqs. (4) and (7) can be approximated by the first two terms of its Taylor series (parabolic approximation):

$$[1 - \lambda^2(v_x^2 + v_y^2)]^{1/2} \approx 1 - \frac{1}{2} \lambda^2(v_x^2 + v_y^2). \quad (11)$$

Using this approximation, which is equivalent to using Fresnel diffraction, and Eq. (10), the function  $G$  of Eq. (7) can be expressed as

$$G(x, y, z = z_0) = \varphi \int_{-\infty}^{+\infty} \int_{-\infty}^{+\infty} \tilde{g}(v_x, v_y) \exp[-\pi i z_0 \lambda (v_x^2 + v_y^2)] \exp[2\pi i(v_x x + v_y y)] dv_x dv_y = \frac{\varphi}{p^2} \sum_{k=-\infty}^{+\infty} \sum_{l=-\infty}^{+\infty} \exp\left(-\pi i z_0 \lambda \frac{k^2 + l^2}{p^2}\right) \times \exp\left(2\pi i \frac{kx + ly}{p}\right), \quad (12)$$

where the phase factor  $\varphi = \exp(2\pi i z_0/\lambda)$  was introduced.

It is also well known that the fractional Talbot planes of the foci are at<sup>1</sup>

$$z_0 = \left(Q + \frac{M}{N}\right) \frac{2p^2}{\lambda} = \left(Q + \frac{M}{N}\right) z_T, \quad (13)$$

where  $Q, M,$  and  $N$  are natural numbers ( $M < N, N > 0$ ) and  $z_T$  is the Talbot distance. Thus, the function  $G$  in the fractional Talbot planes is

$$G\left[x, y, z = \left(Q + \frac{M}{N}\right) z_T\right] = \frac{\varphi}{p^2} \sum_{k=-\infty}^{+\infty} \sum_{l=-\infty}^{+\infty} \exp\left[-2\pi i \frac{M}{N} (k^2 + l^2)\right] \times \exp\left(2\pi i \frac{kx + ly}{p}\right). \quad (14)$$

By dividing the sums into  $N$  sums via the index transformations

$$k = Nk' + m, \quad (15)$$

$$l = Nl' + n, \quad (16)$$

with  $k'$  and  $l'$  integer numbers and  $m, n \in \{0, \dots, N-1\}$ , Eq. (14) can be written as

$$\begin{aligned}
 G\left[x,y,z=\left(Q+\frac{M}{N}\right)z_T\right] &= \frac{\varphi}{p^2} \sum_{m=0}^{N-1} \sum_{n=0}^{N-1} \exp\left\{2\pi i\left[\frac{mx+ny}{p} - \frac{M}{N}(m^2+n^2)\right]\right\} \\
 &\times \sum_{k'=-\infty}^{+\infty} \sum_{l'=-\infty}^{+\infty} \exp\left(2\pi i N \frac{k'x+l'y}{p}\right). \quad (17)
 \end{aligned}$$

Using Eq. (8) with a reduced period  $p/N$ , this becomes

$$\begin{aligned}
 G\left[x,y,z=\left(Q+\frac{M}{N}\right)z_T\right] &= \frac{\varphi}{N^2} \sum_{m=0}^{N-1} \sum_{n=0}^{N-1} \exp\left\{2\pi i\left[\frac{mx+ny}{p} - \frac{M}{N}(m^2+n^2)\right]\right\} \\
 &\times \sum_{k=-\infty}^{+\infty} \sum_{l=-\infty}^{+\infty} \delta\left(x-k\frac{p}{N}\right)\delta\left(y-l\frac{p}{N}\right). \quad (18)
 \end{aligned}$$

Thus, the function  $G$  is a sum of weighted  $\delta$  peaks with the reduced period  $p/N$ . Finally, using Eq. (6), the wave amplitude in the fractional Talbot planes results in

$$\begin{aligned}
 u\left[x,y,z=\left(Q+\frac{M}{N}\right)z_T\right] &= \varphi \sum_{k=-\infty}^{+\infty} \sum_{l=-\infty}^{+\infty} F_{k,l,M,N} A\left(x-k\frac{p}{N}, y-l\frac{p}{N}\right), \quad (19)
 \end{aligned}$$

with the complex factor

$$\begin{aligned}
 F_{k,l,M,N} &= \frac{1}{N^2} \sum_{m=0}^{N-1} \sum_{n=0}^{N-1} \exp\left(2\pi i \frac{km+ln-M(m^2+n^2)}{N}\right) \\
 &= \left[\frac{1}{N} \sum_{m=0}^{N-1} \exp\left(2\pi i \frac{km-Mm^2}{N}\right)\right] \left[\frac{1}{N} \sum_{n=0}^{N-1} \exp\left(2\pi i \frac{ln-Mn^2}{N}\right)\right] \\
 &=: f_{k,M,N} f_{l,M,N}. \quad (20)
 \end{aligned}$$

The complex factor  $F$  is, e.g., responsible for the fact that in the half Talbot plane the foci are not multiplied but only shifted by half a period  $p$  because  $f$  is, in this case, zero for even numbers  $k$  or  $l$ . Note that the theory up to here is valid not only if  $A$  is the wave amplitude of one focus of the microlens array but also if it is an arbitrary function that is repeated after a period  $p$  in the  $x$  and  $y$  direction and that is positioned in a plane at  $z=0$ .

It is very interesting to examine the influence of  $F$  and  $A$  on the intensity height of the multiplied foci in the fractional Talbot planes. If  $A$  is different from zero in only a

small range compared to the reduced period  $p/N$ , there will be no overlap between the multiplied functions  $A$  and the intensity of the peaks will be proportional to  $|F|^2$ . On the other side, if  $A$  is different from zero in a range comparable to  $p/N$  or larger than  $p/N$  the shifted functions  $A(x-kp/N, y-lp/N)$  will overlap, and the resulting wave amplitude is dependent on the complex factor  $F$  and  $A$  itself.

As an example, the 1/4 Talbot plane is discussed. In this case, where  $M=1$  and  $N=4$ , the factor  $f_{k,M,N}$  is

$$\begin{aligned}
 f_{k,1,4} &= \frac{1}{4} \sum_{m=0}^3 \exp\left[i\frac{\pi}{2}m(k-m)\right] \\
 &= \begin{cases} \frac{1}{2}(1-i) & \text{for } k=0 \\ 0 & \text{for } k=1 \\ \frac{1}{2}(1+i) & \text{for } k=2 \\ 0 & \text{for } k=3. \end{cases} \quad (21)
 \end{aligned}$$

Assuming the case that the function  $A$  is rotational symmetric and only different from zero for  $x^2+y^2 \leq (p/2)^2$ , because of symmetry we must distinguish between three different kinds of foci in the 1/4 Talbot plane. The complex amplitude in the center of each of these foci is

$$\begin{aligned}
 u(0,0,z=\frac{1}{4}z_T) &= \varphi \left[ \frac{1}{4}(1-i)^2 A(0,0) + (1-i)(1+i) A\left(\frac{p}{2},0\right) \right] \\
 &= \varphi \left[ -\frac{1}{2}i A(0,0) + 2A\left(\frac{p}{2},0\right) \right], \quad (22)
 \end{aligned}$$

$$\begin{aligned}
 u\left(\frac{p}{2},0,z=\frac{1}{4}z_T\right) &= \varphi \left\{ \frac{1}{4}(1-i)(1+i)A(0,0) + \frac{1}{2}[(1-i)^2 \right. \\
 &\quad \left. + (1+i)^2]A\left(\frac{p}{2},0\right) \right\} = \frac{1}{2}\varphi A(0,0), \quad (23)
 \end{aligned}$$

$$\begin{aligned}
 u\left(\frac{p}{2},\frac{p}{2},z=\frac{1}{4}z_T\right) &= \varphi \left[ \frac{1}{4}(1+i)^2 A(0,0) + (1-i) \right. \\
 &\quad \left. \times (1+i)A\left(\frac{p}{2},0\right) \right] \\
 &= \varphi \left[ \frac{1}{2}i A(0,0) + 2A\left(\frac{p}{2},0\right) \right]. \quad (24)
 \end{aligned}$$

For the complex numbers,

$$A(0,0) = a \exp(i\alpha) \quad \text{and} \quad A\left(\frac{p}{2},0\right) = b \exp(i\beta), \quad (25)$$

the intensity in the foci is

$$|u(0,0,z = \frac{1}{4} z_T)|^2 = \frac{1}{4} a^2 + 4b^2 + 2ab \sin(\alpha - \beta), \quad (26)$$

$$\left| u\left(\frac{p}{2}, 0, z = \frac{1}{4} z_T\right) \right|^2 = \frac{1}{4} a^2, \quad (27)$$

$$\left| u\left(\frac{p}{2}, \frac{p}{2}, z = \frac{1}{4} z_T\right) \right|^2 = \frac{1}{4} a^2 + 4b^2 - 2ab \sin(\alpha - \beta). \quad (28)$$

From these considerations it is obvious that the heights of the foci will be different in the 1/4 Talbot plane if  $b$  [which means  $A(p/2,0)$ ] is different from zero. It is also quite interesting that the height also depends on the phase difference  $\alpha - \beta$ . Similar but more complex calculations can be done for the other fractional Talbot planes.

### 3 Numerical Simulations

In principle, Eq. (19) can be used to calculate directly the complex wave amplitude and intensity in the fractional Talbot planes. But there are two drawbacks. First, to use Eq. (19) the complex wave amplitude  $A(x,y)$  of a single microlens in the focal plane must be known. This requires numerical calculations if the wave aberrations of the lens and light that misses the lens because of its circular aperture must also be considered. For ideal diffractive lenses with quadratic aperture this would be of course not necessary. Second, for the derivation of Eq. (19) the approximation of the square root [Eq. (11)] in the exponent of the propagation phase factor by the first two terms of its Taylor series was used. This is valid only if the spatial frequencies are small. For lenses with high numerical apertures the square root must be calculated exactly, and Eq. (19) is no longer valid.

We have therefore included the latest version of our optical analysis and design program<sup>7</sup> RAYTRACE 6.0 in the following direct method for the numerical calculations. The microlens array with period  $p$  in the  $x$  and  $y$  directions is represented by one microlens. The complex wave amplitude  $A_0(x,y)$  in a plane just behind the microlens is calculated using optical path length calculations via ray tracing and by assuming that the modulus of the wave amplitude is constant. Here  $A_0$  is computed at a square grid of  $N \times N$  points with a total size  $p \times p$  of the field, where  $N = 2^n$  is a power of two. The Fourier transform  $\bar{A}_0$  of  $A_0$  is calculated via a fast Fourier transformation<sup>8</sup> (FFT). Thus, it must be guaranteed that  $N$  is large enough to avoid aliasing effects in the frequency domain. With  $N$  points and a diameter  $p$  of the field the maximum spatial frequency  $v_{\max}$  and the maximum numerical aperture  $NA_{\max}$  of  $\bar{A}_0$ , which can be presented for a wavelength  $\lambda$ , is

$$v_{\max} = \frac{N}{2p} \Rightarrow NA_{\max} = \lambda v_{\max} = \frac{N\lambda}{2p}. \quad (29)$$

If  $NA_{\max}$  is about twice the NA of the lens aliasing effects can be neglected, this is also so if wave aberrations are present.

After this,  $\bar{A}_0$  is multiplied by the propagation phase factor [Eq. (4)]:

$$\bar{A}_{\text{prop}}(v_x, v_y) = \bar{A}_0(v_x, v_y) \exp \left\{ 2\pi i \frac{z}{\lambda} \left[ 1 - \lambda^2 (v_x^2 + v_y^2) \right]^{1/2} \right\}, \quad (30)$$

where  $z$  is the distance of the propagation. If the wave must be propagated to a fractional Talbot plane with parameters  $Q$ ,  $M$ , and  $N$  [see Eq. (13)] and if  $f$  is the focal length of the microlens the distance  $z$  must be

$$z = f + z_0 = f + \left( Q + \frac{M}{N} \right) \frac{2p^2}{\lambda}. \quad (31)$$

The resulting function  $\bar{A}_{\text{prop}}$  in the frequency domain is then transformed back to the spatial domain by an inverse FFT. There, the aliasing effects, which are normally undesirable, are essential. They cause the wave amplitudes that would lie outside one period to be projected into the period, simulating an infinitely extended periodic array of microlenses with period  $p$  in the  $x$  and  $y$  directions.

A simulation for planoconvex refractive microlenses made of photoresist was performed (see Figs. 2 and 3). The microlenses are illuminated by a plane wave with the plane side of the lens toward the plane wave, which is the most common situation for microlenses because of their small focal lengths. The parameters for the simulation are period of the microlens array  $p = 100 \mu\text{m}$ , diameter of a single lens  $d = 80 \mu\text{m}$ , focal length of each lens  $f = 130 \mu\text{m}$ , wavelength of the illuminating plane wave  $\lambda = 633 \text{ nm}$ , and number of points for the calculation  $N \times N = 512 \times 512$ .

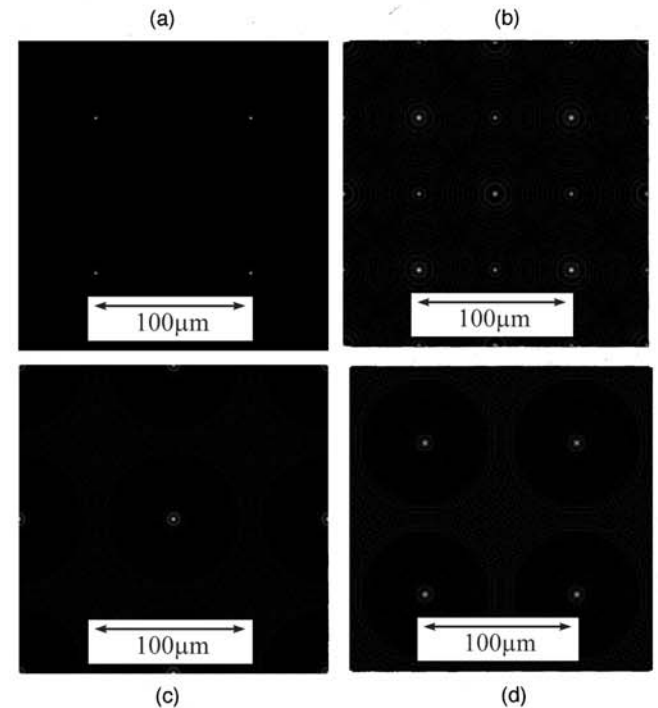


**Fig. 2** Results of the simulation for a microlens array with 100- $\mu\text{m}$  period, 80- $\mu\text{m}$ -diam of each lens, and 130- $\mu\text{m}$  focal length illuminated at a 633-nm wavelength: (a) 0 Talbot plane, (b) 1/4 Talbot plane, (c) 1/2 Talbot plane, and (d) 1 Talbot plane.

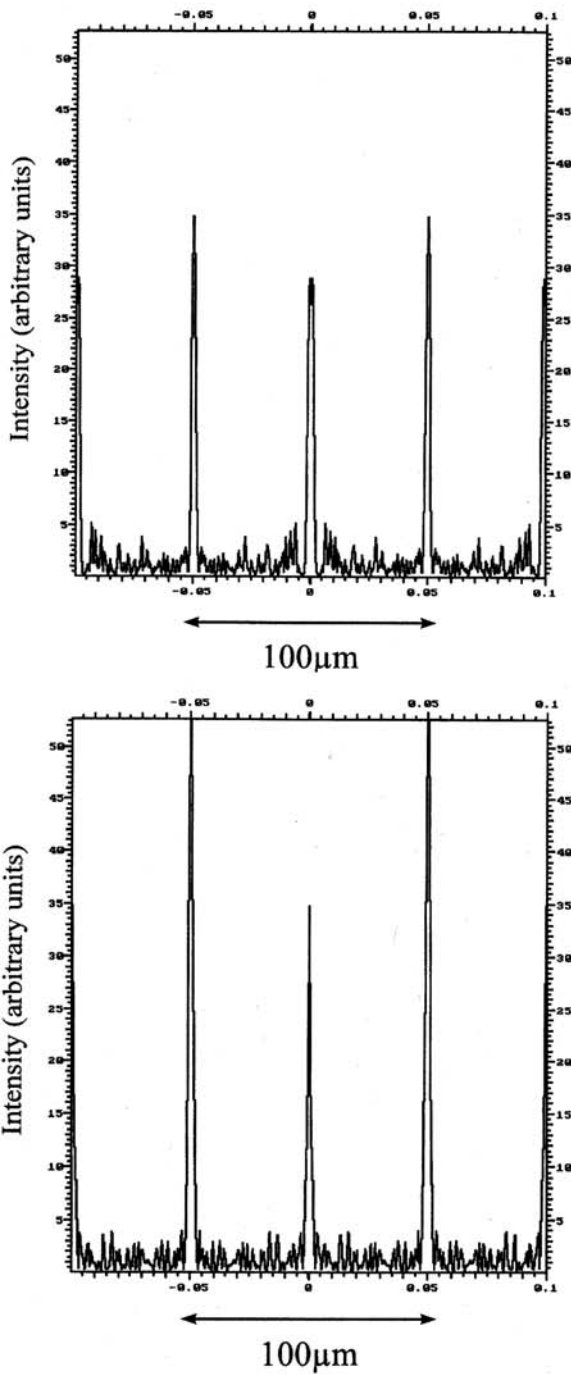


**Fig. 3** Sections through the foci in the 1/4 Talbot plane for two neighboring lines of the foci with a distance of  $p/2$  (simulation). The doubled foci for each line have different heights.

The intensity peaks of the doubled foci with the distance  $p/2$  in the 1/4 Talbot plane have different heights (Fig. 3). It is noteworthy that the ratio of the absolute values of the intensity peaks between the 0 Talbot plane (focal plane) and the 1/2 Talbot plane is about 14 and between the 0 Talbot plane (focal plane) and the 1 Talbot plane about 20. The  $z$  positions of the foci, which means where the peaks have maximum heights, are shifted slightly toward the microlens array compared to the values calculated with Eq.

(31) for the different fractional Talbot planes ( $100 \mu\text{m}$  for the 1 Talbot plane,  $90 \mu\text{m}$  for the 1/2 Talbot plane, and  $30 \mu\text{m}$  for the 1/4 Talbot plane). The axial shift due to the spherical aberration of the lenses was thereby considered separately. Both of these effects are a consequence of the large NAs of the lenses so that the parabolic approximation of the square root in the exponent of the propagation factor, which was used in Sec. 2, is no longer valid.

In all considerations to here, walk-off effects were neglected. These are no longer negligible if the number of lenses of an array is small or if foci at the edge of an array are considered. In principle, it is also possible to simulate walk-off effects with our numerical method if the complex amplitude behind a whole array of lenses that is embedded in an area of diameter  $D$  with constant or zero complex amplitude is propagated. The diameter  $D$  must be so large that aliasing effects can be neglected. If  $D_0$  is the diameter of the lens array and the lenses have a particular NA, then the diameter  $D$  to propagate along a distance  $z$  must be at least

$$D \approx D_0 + 2z\text{NA}. \tag{32}$$

If NA is large or the aberrations of the lenses are present,  $D$  must be still larger to avoid aliasing effects. In practice, this is possible only for arrays with a few lenses and small NAs because Eq. (29), where  $p$  must be replaced by  $D$ , must be fulfilled. If  $D_0$  can be neglected, the number  $N$  of points for the calculation increases with the square of the NA of the lenses. Therefore,  $N$  will exceed the memory capacity and computing speed of actual computers for large NAs.

Figure 4 shows the simulation of a  $6 \times 6$  refractive microlens array with  $100\text{-}\mu\text{m}$  period,  $100\text{-}\mu\text{m}$  lens diameter,

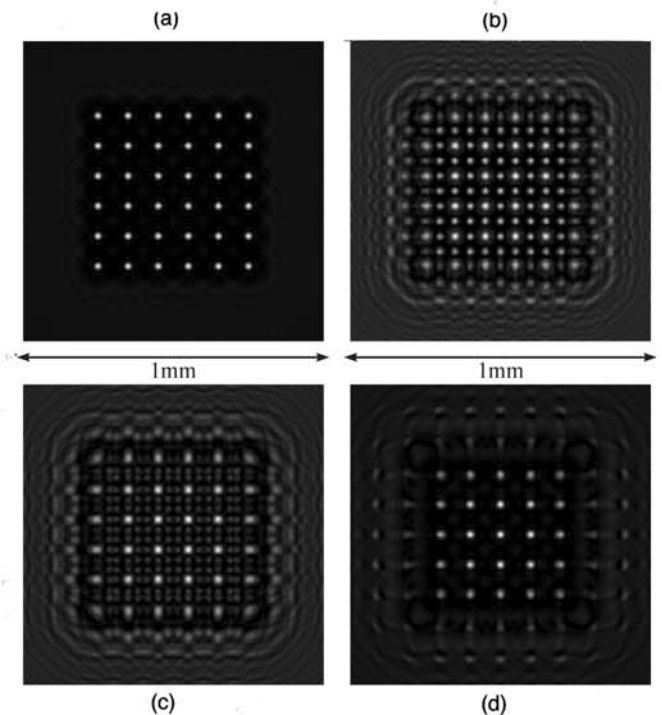


**Fig. 4** Simulation of the foci of a finite microlens array ( $6 \times 6$  lenses) with  $100\text{-}\mu\text{m}$  period,  $100\text{-}\mu\text{m}$  lens diameter,  $2.5\text{-mm}$  focal length, and  $0.633\text{-}\mu\text{m}$  wavelength: (a) 0 Talbot plane (focal plane), (b) 1/4 Talbot plane, (c) 1/3 Talbot plane, and (d) 1/2 Talbot plane.

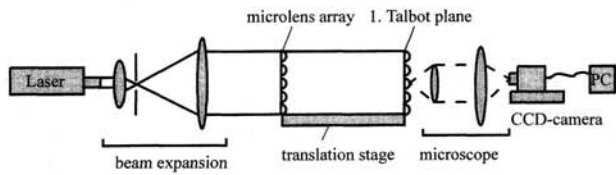


**Fig. 5** Experimental setup. The microlens array is mounted on a translation stage for axial shifts between the fractional Talbot planes. The scheme shows the position for the measurement of the 1 Talbot plane.

and 2.5-mm focal length, i.e.,  $NA=0.02$  and  $\lambda=0.633 \mu\text{m}$ . The total field size in the simulation was  $D=2 \text{ mm}$  with  $N=512$  points. Only the central part of  $1 \times 1 \text{ mm}$  size is shown in the figures. The peak-to-valley values of the intensity are 30% for the 1/4 plane, 36% for the 1/3 Talbot plane, and 72% for the 1/2 Talbot plane compared to the focal plane.

#### 4 Experimental Results

An experimental setup for the measurement of the intensity distribution in the different fractional Talbot planes of a microlens array was built (see Fig. 5). The microlens array, used in the setup has the same paraxial parameters as the array used in the simulations of the last section. The experimental results are shown in Figs. 6 and 7. It can be seen that the foci are broadened compared to the foci of the simulation which is an effect of larger wave aberrations of the real lenses compared to ideal spherical lenses and an effect of misalignment aberrations. Therefore, the light that passes the spacing between the lenses (Fig. 6) is brighter compared to the simulation (Fig. 2). The different heights of the foci in the 1/4 Talbot plane can be seen clearly (Fig. 7) and the relative heights are in quite good agreement with

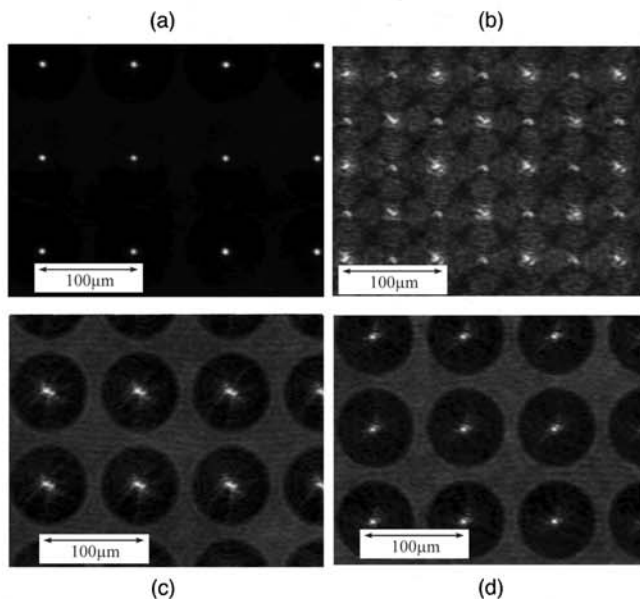


**Fig. 6** Experimental results for a microlens array with 100- $\mu\text{m}$  period, 80- $\mu\text{m}$  diameter of each lens, and about 130- $\mu\text{m}$  focal length illuminated at 633-nm wavelength: (a) 0 Talbot plane, (b) 1/4 Talbot plane, (c) 1/2 Talbot plane, and (d) 1 Talbot plane.

the simulation (Fig. 3). The ratio of the absolute values of the intensity peaks between the 0 Talbot plane (focal plane) and the 1/2 Talbot plane is about 22 and between the 0 Talbot plane (focal plane) and the 1 Talbot plane is about 23 for the experimental results. The  $z$  positions of the foci are also shifted slightly toward the microlens array compared to the theoretical positions of the parabolic approximation of Sec. 2 (130  $\mu\text{m}$  for the 1 Talbot plane, 120  $\mu\text{m}$  for the 1/2 Talbot plane, and 50  $\mu\text{m}$  for the 1/4 Talbot plane). These results are also in quite good agreement with the numerical simulation.

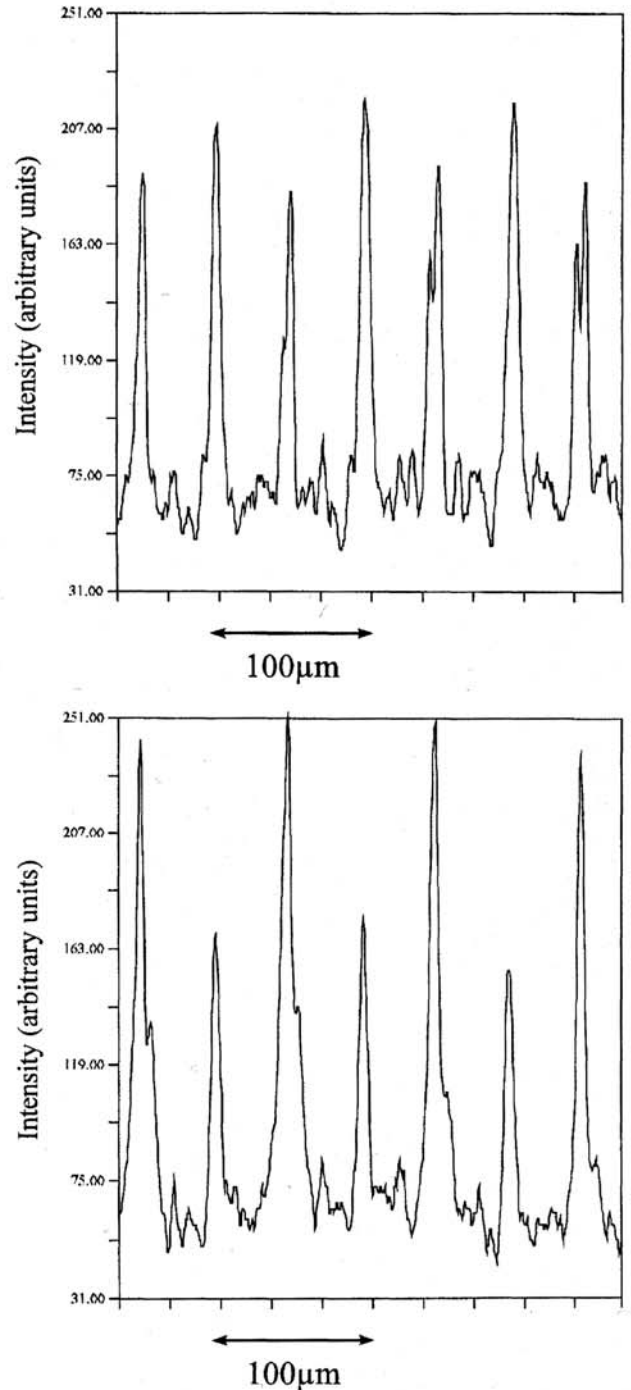


**Fig. 7** Sections through the foci in the 1/4 Talbot plane for two neighboring lines of the foci with a distance of  $p/2$  (experimental results). The doubled foci for each line have different heights.

## 5 Conclusion

It has been shown in this paper that the fractional Talbot effect for the foci of microlens arrays is a quite complex phenomenon. Analytic expressions for the simplified case of small spatial frequencies, which means small lens NAs, were given in Sec. 2. Especially, the dependence of the height of the foci in the  $1/4$  Talbot plane on the complex amplitude function of a single focus was discussed. A numerical method for the simulation of the fractional Talbot effect was described in Sec. 3. This method is also valid for large spatial frequencies, which are present in the case of microlenses with a high NA. The quite good agreement between this simulation method and experimental results was shown in Sec. 4.

## References

1. J. T. Winthrop and C. R. Worthington, "Theory of Fresnel images. I. Plane periodic objects in monochromatic light," *J. Opt. Soc. Am.* **55**(4), 373-381 (1965).
2. W. D. Montgomery, "Self-imaging objects of infinite aperture," *J. Opt. Soc. Am.* **57**(6), 772-778 (1967).
3. E. Bonet, P. Andres, J. C. Barreiro, and A. Pons, "Self-imaging properties of a periodic microlens array: versatile array illuminator realization," *Opt. Commun.* **106**, 39-44 (1994).
4. N. Streibl, "Beam shaping with optical array generators," *J. Mod. Opt.* **36**(12), 1559-1573 (1989).
5. A. W. Lohmann, "Array illuminators and complexity theory," *Opt. Commun.* **89**, 167-172 (1992).
6. J. W. Goodman, "The angular spectrum of plane waves," Chap. 3.7 in *Introduction to Fourier Optics*, pp. 48-54, McGraw-Hill, New York (1968).
7. N. Lindlein, *RAYTRACE 6.0: Optical Analysis and Design Software*, Distributed by MIKOS, Weichselgarten (1996).
8. W. H. Press, B. P. Flannery, S. A. Teukolsky, and W. T. Vetterling, "Fourier transform spectral methods," Chap. 12 in *Numerical Recipes in C*, pp. 398-470, Cambridge University Press, Cambridge (1991).



**Brigitte Besold** is studying physics at the University of Erlangen-Nürnberg, Germany, where she is currently finishing her diploma work on the fractional Talbot effect for microlens arrays.



**Norbert Lindlein** studied physics at the University of Erlangen-Nürnberg, Germany, where he received his diploma degree in 1992 and his PhD in 1996. His research interests include the analysis and design of optical systems, holography, and micro-optics.